Particuology 13 (2014) 128–133

Contents lists available at ScienceDirect

Particuology

journal homepage: www.elsevier.com/locate/partic

Transition of axial segregation patterns in a long rotating drum

Zequn Cui[a], Yongzhi Zhao[a,*], Youchuan Chen[a,b], Xiao Liu[a], Zhengli Hua[a], Chilou Zhou[a], Jinyang Zheng[a]

[a] State Key Laboratory of Chemical Engineering, Institute of Process Equipment, Department of Chemical and Biochemical Engineering, Zhejiang University, Hangzhou 310027, China

[b] Institute of Coal Chemistry, Chinese Academy of Sciences, Taiyuan 030001, China

ARTICLE INFO

Article history:
Received 26 September 2012
Received in revised form
22 November 2012
Accepted 5 February 2013

Keywords:
Long rotating drum
Discrete element method
Axial segregation pattern
End wall effect
Rotational speed

ABSTRACT

Axial segregation of a bidisperse mixture of particles in a long rotating drum is studied using the discrete element method. Simulation results show that particle interaction is responsible for axial segregation, the patterns of which are influenced by the end wall effect. Axial segregation patterns transform under competing influences of the end walls and the particle interaction forces. The two influential factors vary with various rotational speeds and end wall friction levels. The result is the transition of different axial segregation patterns: two large-particle bands at both ends, two small-particle bands at both ends, or a random segregation pattern where either a large-particle band or small-particle band may appear at either end.

1. Introduction

Axial segregation in a long rotating drum partially filled with a bidisperse mixture of small and large particles is an intriguing phenomenon that has aroused the interest of many researchers (Aranson & Tsimring, 2006; Arndt, Siegmann-Hegerfeld, Fiedor, Ottino, & Lueptow, 2005; Chen, Lochman, Ottino, &Lueptow, 2009; Chen, Ottino & Lueptow, 2010; Choo, Baker, Molteno, & Morris, 1998; Fiedor & Ottino, 2003; Hill & Kakalios, 1994, 1995; Jain, Khakhar, Lueptow, & Ottino, 2001; Juarez, Ottino & Lueptow, 2008; Maneval, Hill, Smith, Caprihan, & Fukushima, 2005; Nguyen, Sederman, Mantle, & Gladden, 2011; Pohlman, Ottino & Lueptow, 2006; Rapaport, 2002; Richard & Taberlet, 2008; Taberlet, Newey, Richard, & Losert, 2006; Zik, Levine, Lipson, Shtrikman, & Stavans, 1994). Once rotation starts, the mixture quickly acquires a pattern of alternative bands of mostly large or small particles; this applies to a wide range of conditions (Hill & Kakalios, 1994, 1995; Jain et al., 2001; Zik et al., 1994). Large particles first converge at the ends of the drum (Fiedor & Ottino, 2003; Hill & Kakalios, 1994; Juarez et al., 2008), showing a normal axial segregation pattern. The end walls play a significant role in the axial segregation pattern as the granular flow near the end walls is different from the flow far from them (Maneval et al., 2005; Pohlman, Ottino, et al., 2006). Influenced by the friction of the end walls, particles close to the end walls attain higher velocities (Pohlman, Ottino, et al., 2006) while the surface particles flow away from the end walls upstream and curve back toward the end walls downstream because of mass conservation (Chen, Ottino & Lueptow, 2008; Maneval et al., 2005; Pohlman, Meier, Lueptow, & Ottino, 2006; Pohlman, Ottino, et al., 2006; Santomaso, Olivi, & Canu, 2004). Small particles are entrapped in the body of the particle bed far from the end walls because of the radial segregation, resulting in large particles accumulating at the ends (Chen et al., 2010). Thus, the end walls have a considerable effect on axial segregation; however, opinions still differ on whether end wall effect is the primary factor (Chen et al., 2010; Choo, Molteno, & Morris, 1997; Zik et al., 1994).

The large-particle bands appear at the ends of the drum because of the frictional influence of the end walls. One question therefore arises: how would low-friction end walls affect the particle behavior in a rotating drum? In our numerical simulations, we varied the friction coefficients between the end walls and the particles from 0 to 1 at a series of rotational speeds of the drum. We found that additional axial segregation patterns may appear at low end wall friction.

2. Mathematical model

In the discrete element model, particle movement is described by Newton's equation of motion, which includes the effects of gravity and contact force. For a particle with mass m and moment

* Corresponding author. Tel.: +86 13185087060.
E-mail address: yzzhao@zju.edu.cn (Y. Zhao).

1674-2001/$ – see front matter © 2013 Chinese Society of Particuology and Institute of Process Engineering, Chinese Academy of Sciences. Published by Elsevier B.V. All rights reserved.
http://dx.doi.org/10.1016/j.partic.2013.02.013

of inertia I, the equations of translation and rotation can be written as

$$m\frac{d\boldsymbol{v}}{dt} = m\boldsymbol{g} + \sum \boldsymbol{F}_{\mathrm{c}}, \tag{1}$$

$$I\frac{d\boldsymbol{\omega}}{dt} = \sum \boldsymbol{T}_{\mathrm{c}}, \tag{2}$$

where the translational motion of the particle is a function of the sum of the forces acting on the particle while the rotational motion of the particle depends on the contact torque acting on it. In Eqs. (1) and (2), $d\boldsymbol{v}/dt$ represents the acceleration of the translational motion of the particle, $\boldsymbol{g}$ is the gravitational acceleration, and $d\boldsymbol{\omega}/dt$ represents the angular acceleration of the rotational motion of the particle. The contact force $\boldsymbol{F}_{\mathrm{c}}$ is composed of the normal contact force $\boldsymbol{F}_{\mathrm{c,n}}$ and the tangential contact force $\boldsymbol{F}_{\mathrm{c,t}}$:

$$\boldsymbol{F}_{\mathrm{c}} = \boldsymbol{F}_{\mathrm{c,n}} + \boldsymbol{F}_{\mathrm{c,t}} \tag{3}$$

The contact torque $\boldsymbol{T}_{\mathrm{c}}$ combines the torque $\boldsymbol{T}_{\mathrm{t}}$ generated by the tangential contact force and the rolling friction torque $\boldsymbol{T}_{\mathrm{r}}$:

$$\boldsymbol{T}_{\mathrm{c}} = \boldsymbol{T}_{\mathrm{t}} + \boldsymbol{T}_{\mathrm{r}} \tag{4}$$

The contact forces and torques between two spherical particles can be obtained by the three-equation linear spring–dashpot model, which was first proposed by Cundall and Strack (1979) and improved by Iwashita and Oda (1998). The model estimates the contact forces using the linear spring, dashpot, and friction slider, where the parameters of the spring constants, the damping coefficients, and the friction coefficients can be obtained from the physical properties of the particles and the computational conditions (Zhao, Jiang, Liu, & Zheng, 2009; Zhao, Cheng, Wu, Ding, & Jin, 2010; Zhao, Ding, Wu, & Cheng, 2010). The normal and tangential contact forces and the rolling friction torque are given by

$$\boldsymbol{F}_{\mathrm{c,n}} = -k_{\mathrm{n}}\boldsymbol{\delta}_{\mathrm{n}} - \eta_{\mathrm{n}}\boldsymbol{v}_{\mathrm{n}}, \tag{5}$$

$$\boldsymbol{F}_{\mathrm{c,t}} = -k_{\mathrm{t}}\boldsymbol{\delta}_{\mathrm{t}} - \eta_{\mathrm{t}}\boldsymbol{v}_{\mathrm{t}}, \tag{6}$$

$$\boldsymbol{T}_{\mathrm{r}} = -k_{\mathrm{r}}\boldsymbol{\alpha} - \eta_{\mathrm{r}}\boldsymbol{\omega}, \tag{7}$$

where $\boldsymbol{\delta}_{\mathrm{n}}$ and $\boldsymbol{\delta}_{\mathrm{t}}$ are the particle displacements in the normal and tangential directions, respectively, $\boldsymbol{\alpha}$ is the torsional deformation between the particles, $\boldsymbol{v}_{\mathrm{n}}$ and $\boldsymbol{v}_{\mathrm{t}}$ are the relative velocities of the particles in the normal and tangential directions, respectively, $\boldsymbol{\omega}$ is the relative angular velocity of the particles, k is the stiffness of the spring and $\boldsymbol{\eta}$ is the damping coefficient. The subscripts n, t, and r represent normal, tangential, and rolling, respectively. The damping coefficient can be calculated by the equations presented in Ting and Corkum (1992) using the restitution coefficient.

If the following relations are satisfied

$$|\boldsymbol{F}_{\mathrm{c,t}}| > f_{\mathrm{s}}|\boldsymbol{F}_{\mathrm{c,n}}|, \tag{8}$$

$$|\boldsymbol{T}_{\mathrm{r}}| > f_{\mathrm{r}}|\boldsymbol{F}_{\mathrm{c,n}}|, \tag{9}$$

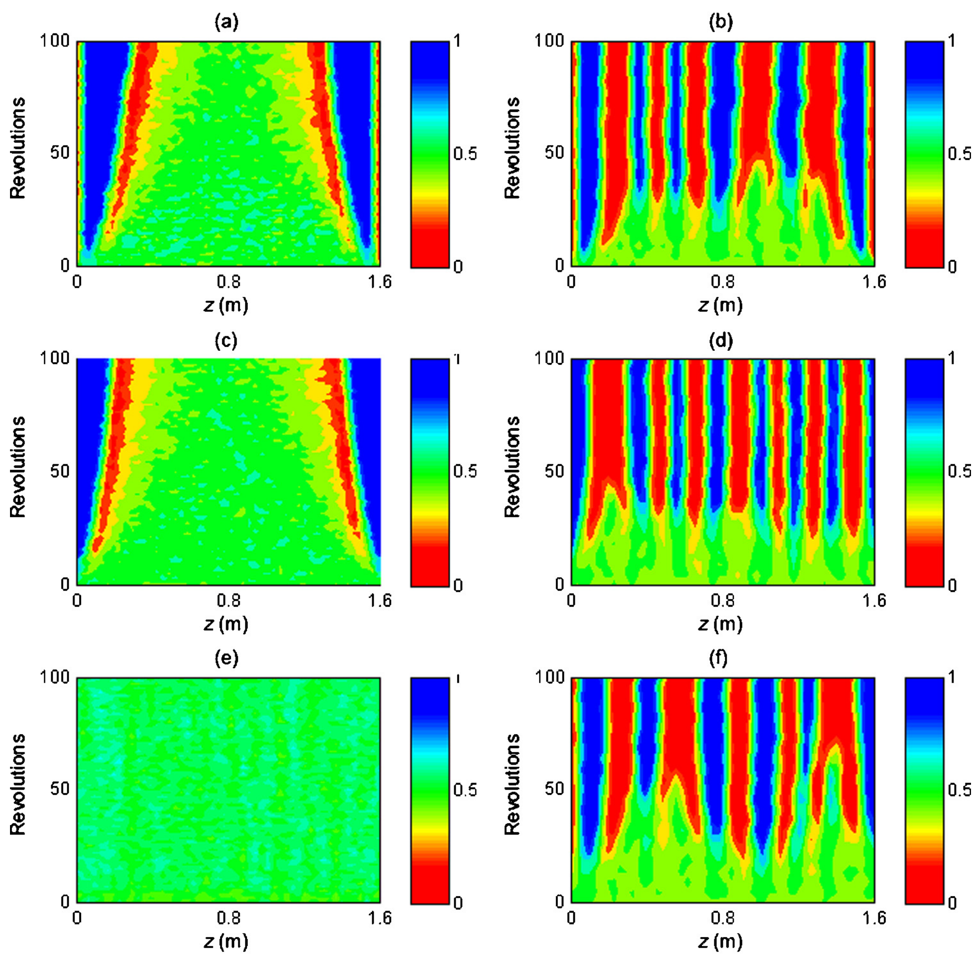

Fig. 1. Space–time plots showing the evolution of axial segregation at different rotational speeds, Ω = 1 rad/s (left column) and Ω = 3 rad/s (right column), with rough end walls (a) and (b) ($f_s^{wp} = 0.6$), frictionless end walls (c) and (d) ($f_s^{wp} = 0$), and transitional end wall friction (e) ($f_s^{wp} = 0.025$) and (f) ($f_s^{wp} = 0.01$), respectively. Red and blue color presents districts rich in large particles and small particles, respectively, while green color presents districts where particles mixed well and the interfaces of large-particle bands and small-particle bands. (For interpretation of the references to color in this figure legend, the reader is referred to the web version of the article.)